Nanotechnology Perceptions
ISSN 1660-6795
www.nano-ntp.com

Early Diagnosis of Breast Cancer Feature Extraction and Classification Using CNNs with Alexnet and Cascaded VGG19

M. Subha[1], Dr. P. Srimanchari[2]

[1]Ph.D Research Scholar, Department of Computer Science, Erode Arts and Science College (Autonomous), India.
[2]Assistant Professor, Department of Computer Science, Erode Arts and Science College (Autonomous), India

Breast cancer is a significant health concern globally, emphasizing the need for effective early diagnosis methods. In this research, we proposed a novel approach for early breast cancer detection that utilizing deep learning techniques. Specifically, we utilize Convolutional Neural Networks (CNNs) with two distinct architectures: AlexNet for feature extraction and Cascaded VGG19 for classification. The first stage of our approach involves feature extraction using the AlexNet architecture. This CNN is pre-trained on large-scale image datasets, enabling it to extract meaningful and discriminative features from breast cancer images. These extracted features serve as a high-level representation of the underlying characteristics of the tumors, aiding in subsequent classification tasks. In the second stage, we employ a cascaded VGG19 architecture for classification purposes. The cascaded VGG19 model is fine-tuned on the extracted features from AlexNet and trained to differentiate between malignant and benign breast cancer cases. This tailored classification model enhances the accuracy and reliability of early breast cancer diagnosis.

Keywords: Breast cancer,Cascaded VGG19,Convolutional Neural Networks, deep learning, early diagnosis.

1. Introduction

The huge effects of breast cancer on both people and healthcare systems mean that it remains a major global health concern [1]. The survival rate and treatment success rate of breast cancer patients are greatly improved when the disease is detected early on [2]. When it comes to identifying benign from malignant tumors and detecting minor abnormalities, traditional diagnostic procedures like mammography and ultrasound aren't very good [3-4]. A lot of people have been thinking about how to use deep learning and CNNs to improve breast cancer detection in the early stages recently [5]. When it comes to picture analysis and pattern identification, deep learning methods, and CNNs in particular, have shown to be quite effective [6]. The ability of these models to learn hierarchical data representations on their own makes

them ideal for complicated feature extraction from medical pictures, such as breast tumor images [7-8]. Researchers have improved breast cancer diagnosis methods by using CNNs, which are more powerful and accurate [9].

Cancer of the breast, which affects a disproportionate number of women, begins in the breast's cells. Breast cancer is second only to lung cancer in terms of the percentage of female patients who succumb to the disease [10]. Fortunately,Ductal carcinoma in situ(DCIS) usually advances at a modest pace and has little to no effect on patients' regular life [11, 12]. The DCIS form accounts for a small number of instances (between 20% and 53%), whereas the IDC type encases the whole breast tissue and is more harmful [13]. This group comprises over 80% of breast cancer patients. Patients and their device's electronic medical records are part of healthcare technology, which also includes their retrieval and maintenance [14]. The identification of cancer has long been a problem in the field of hematological illness diagnosis and therapy. A large portion of the population is now dealing with health issues [15]. The field of medicine has made remarkable strides in recent years. Even with all these improvements, the general population still knows very little about health and illness [16-18]. Many people probably deal with health problems, and some of those problems might be deadly. By implementing safe, realistic procedures and making use of contemporary technology, we can not only improve the accuracy of the early diagnosis of deadly diseases, but also decrease the total cost of health care and the need for caretakers. Intelligent decision-making techniques and technology that are up-to-date might potentially save several lives [19–21].

The main contribution of the paper is

- Feature extraction using CNN with Alexnet
- Classification using cascaded VGG 19

This paper is organized as follows for the rest of it. Several writers discuss several methods for detecting breast cancer in Section 2. In Section 3, we can see the suggested model. In Section 4, we outline the results of the inquiry. Section 5 discusses the results and possible directions for further study.

1.1 Motivation of the paper

The motivation of this paper lies in addressing the critical need for effective early detection methods for breast cancer, a significant global health concern. By utilizing advanced deep learning techniques, specifically CNNs with AlexNet for feature extraction and Cascaded VGG19 for classification, we aim to improve the accuracy and reliability of early breast cancer diagnosis. Our approach capitalizes on the capabilities of pre-trained models and large-scale image datasets to extract meaningful features and differentiate between malignant and benign cases. Through comprehensive experimentation and evaluation, we demonstrate the efficacy of our CNN-based approach in achieving high accuracy and sensitivity in detecting breast cancer at an early stage, ultimately contributing to enhanced patient outcomes and treatment strategies.

2. Background Study

Abdelrahman, L.et al. [1] important gaps in the current body of knowledge were highlighted

throughout the literature. Knowledge from more extensive, well-annotated datasets can be applied to sparser ones with the aid of transfer learning. Additional investigation was necessary to determine its applicability to the breast asymmetry detection task. This method calls for more annotated datasets, therefore researchers should concentrate on building large corpora in the future.

Alanazi, S.et al. [4] Improving health care via automated breast cancer screening was no easy feat. , To automatically diagnose this malignancy, the present research suggests a CNN method that examines the IDC tissue areas in Whole Blood Samples (WSIs).

Amrane, M.et al. [8] these authors' findings indicate that the Light GBM method performs well on diagnostic datasets and was simple to use. The author was able to extract 16 features from a total of 30 after eliminating outliers; these features significantly improved the model's accuracy. With a precision of 97.07%, LightGlioBlastoma Multiforme(GBM) outperformed the other four methods that were considered.

Desai, M., & Shah, M.et al. [10] every member of society relies on the healthcare system to obtain the proper diagnosis and treatment when they need it. Additionally, it conducts studies to counteract emerging viruses, illnesses, and other health problems. Everyone has to take care of their health since it was the single most important aspect in determining their potential.

Gao, F.et al. [12] Breast cancer diagnosis still faces obstacles, one of which was distinguishing benign instances from malignant tumors. This study's contribution was that it uses a Deep-CNN approach to examine the benefits of recombinedContrast-Enhanced Digital Mammography(CEDM) pictures in assisting the identification of breast lesions. The combination of the information provided by conventional FFDM with enhanced features associated with neoangiogenesis makes CEDM an attractive imaging technique (like MRI). These authors literature search revealed no prior research that explored the deep-CNN's potential for CEDM imaging.

Priyanka, K. S. [14] because it was the most common and dangerous cancer, breast cancer detection was a difficult challenge to solve. The survival rate for breast cancer was declining, and the illness was becoming more common each year. Previous studies have shown that machine learning algorithms perform better inside their respective domains.

Tahmooresi, M.et al. [17] an extensive literature review of current ML approaches utilized for breast cancer detection was conducted in this work, which also presented the concepts of breast cancer and ML. Their results imply that Support Vector Machines (SVMs) were the most often employed approach for cancer diagnosis. Either SVM was used alone or in conjunction with another technique to enhance performance.

Table 1: Survey of Breast Cancer Detection Techniques

Author	Year	Methodology	Advantage	Limitation
Abdelrahman et al.	2021	CNN for breast cancer detection in mammography	Comprehensive survey of CNN techniques	Limited focus on other ML approaches
Ajmani et al.	2024	ML and DL techniques for breast cancer detection	Utilization of both ML and DL methods	Limited discussion on specific models
Al-nawashi et al.	2024	ML-based approach for breast cancer detection	New approach in ML-based detection	Lack of comparative analysis

Shah et al.	2024	DCGAN-driven mammogram synthesis for breast cancer dx	Innovative use of DCGAN for synthesis	Limited focus on traditional ML models
Liu et al.	2024	Breast cancer classification using improved VGG16	Improvement in VGG16 for classification	Limited discussion on other networks

2.1 Problem definition

The problem in existing breast cancer detection methodologies lies in their inherent drawbacks, which often delay accurate and reliable early diagnosis. Common drawbacks include limited accuracy in classification tasks, especially in distinguishing between malignant and benign cases, leading to higher false positive or false negative rates. These limitations underscore the need for more advanced and effective approaches, such as deep learning techniques like the VGG16, Improved VGG16, and VGG19 to overcome these challenges and improve early breast cancer detection accuracy.

3. Proposed System

In this section, we describe the proposed methods used in our study for early breast cancer detection. We developed deep learning techniques, specifically CNNs, employing two distinct architectures: AlexNet for feature extraction and Cascaded VGG19 for classification. Initially, AlexNet is utilized to extract meaningful and discriminative features from breast cancer images. These extracted features are then refined and utilized by the cascaded VGG19 model, fine-tuned for classifying between malignant and benign breast cancer cases.

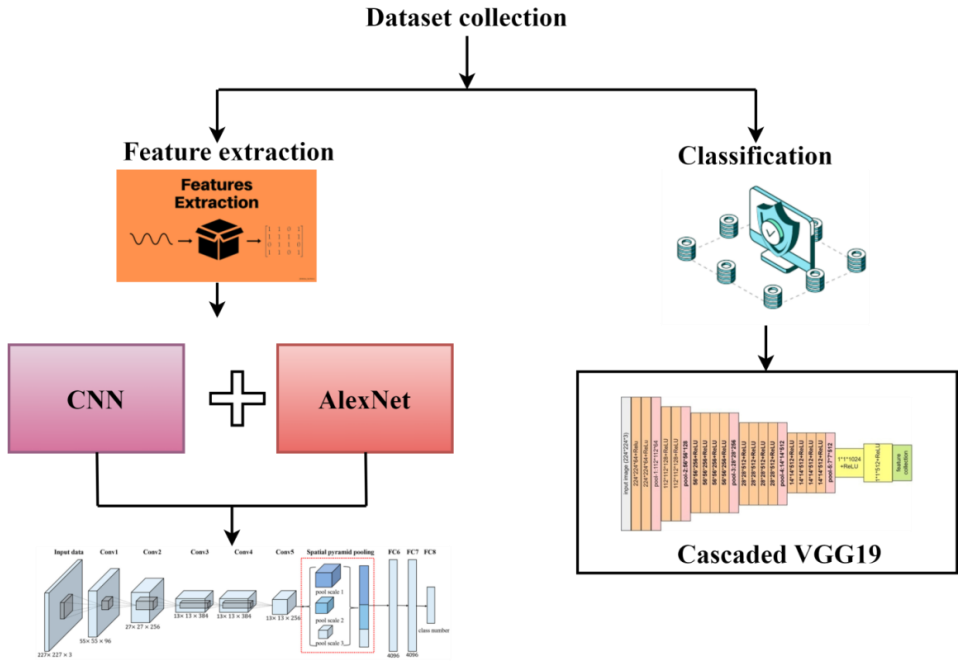

Figure 1: Proposed workflow architecture

3.1 Dataset collection

The dataset has collected from https://data.mendeley.com/datasets/ywsbh3ndr8/2 with 786MB size. The collection includes both benign and malignant tumors seen on mammograms. The 106 INbreast pictures, 53 MIAS photos, and 2188 DDSM images used here were all obtained from other datasets.

3.2 Feature extraction using CNN with Alexnet

Interspersed with sub-sampling layers, convolutional layers decrease computation time while progressively building up more spatial and configural constant referred by Desai, M., & Shah, M. (2021). However, to keep specificity intact, a modest sub-sampling factor is ideal. Though not novel, the notion is profoundly effective despite its apparent lack of originality. These themes are extensively used in models of the mammalian visual cortex. It is still possible that the secret to success in the field of audio analysis lies in hierarchical learning structures.

Let's go ahead and figure out how to derive the back propagation updates for a network's convolutional layers. A number of input maps can be combined into a single output map using convolutions. Overarching, we possess that

$$x_j^l \equiv f\left(\sum_{i\in Mj} x_i^{l-1} * k_{ij}^e + b_j^e\right), \text{--------- (1)}$$

x_j^l: This represents the output of the j^{th} feature map at layer l in the CNN. It's obtained by applying an activation function f to the sum of convolutions between the input maps and corresponding kernels, along with an additive bias b_j^e.

While all-pairs and all-triplets input maps are popular options, we'll talk about learning combinations below. An additive bias b is applied to each output map, but different kernels are convolved into the input maps for each output map.

Every convolution layer 'presumably' is followed by a down sampling layer l+1. The sensitivity of a layer 'unit' in the back propagation algorithm is calculated by summing all the sensitivity values from the layers below it that are linked to units in the current layer that are related with the node of interest. Next, at layer '+ 1, the weights that correspond to each of those connections are specified. Following this, we increase this value by the derivative of the activation function calculated at the pre-activation inputs of the current layer, u. If a down sampling layer follows a convolutional layer, then a single pixel in the following layer's sensitivity map δ will correspond to a group of pixels in the convolutional layer's output map. From the top of the relevant map all the way down to layer '+ 1, there is precisely one unit for every unit. By up sampling the down sampling layer, we can potentially make its sensitivity map as large as the convolutional layer's sensitivity map.

$$\delta_j^l \equiv \beta_j^{l+1}\left(f'\left(u_j^l\right)oup\left(\delta_j^{l+1}\right)\right) \text{---------- (2)}$$

$f'\left(u_j^l\right)$: This term calculates the derivative of the activation function with respect to the pre-activation input u_j^l of the unit in layer l. The derivative f' helps determine how the activation function's output changes concerning changes in the input.

$up(\delta_j^{l+1})$: This term represents the upsampling procedure applied to the sensitivity map δ_j^{l+1} from the next layer. Upsampling involves increasing the size of the input by a factor of n, typically achieved by tiling each input pixel horizontally and vertically n times in the output.

β_j^{l+1}: This is the multiplicative bias associated with the unit in layer l+1. It scales the sensitivity map from the next layer before combining it with the derivative of the activation function and the upsampled sensitivity map.

When the subsampling layer subsamples by a factor of n, the upsampling procedure is simply tiling each input pixel horizontally and vertically n times in the output. Below, we'll talk about how the Kronecker product can be used to efficiently construct this function.

$up(\times) \equiv \times \otimes 1_{n\times n.}$ ---------- (3)

Now that we are aware of the sensitivities for a certain map, we can get the bias gradient rapidly by adding up all the values inδ_j^l.

$\frac{\partial E}{\partial bj} \equiv \sum_{u,v}(\delta_j^l)uv.$ ---------- (4)

$\frac{\partial E}{\partial k_{ij}^l} \equiv \sum_{u,v}(\delta_j^l)uv\left(P_i^{l-1}\right)uv$ ---------- (5)

When this occurs, P_i^{l-1}The resultant convolution map P_i^{l-1} element at (u, v) was calculated by multiplying the patch in $\frac{\partial E}{\partial bj}$ elementwise by ∂k_{ij}^l throughout the convolution process. This eliminates the need to painstakingly record which input map patches go with which output map pixels (and their corresponding sensitivity maps).

$\frac{\partial E}{\partial k_{ij}^l} \equiv \text{rot180}\left(\text{conv2}\left(\times_i^{l-1}, \text{rot180}\left(\delta_j^l\right), '\text{valid}'\right)\right).$ ---------- (6)

Here, we do cross-correlation by rotating the δ_j^l picture rather than convolution. Then, before doing convolution in the feed-forward step, we turn the output backwards to make that the kernel is in the expected orientation.

Maps that have been downsampled are created via a subsampling layer. Despite their reduced size, there will be precisely N output maps for every N input maps. In a more official

$\times_j^l \equiv f\left(\beta_j^l down\left(\times_j^{l-1}\right) + b_j^l\right),$ ---------- (7)

Down (•) is a sub-sampling function. This function usually reduces the input picture by an n-fold in both spatial dimensions by summing over each individual n-by-n block. There is an additive bias b and a multiplicative bias β assigned to each output map. Another option is to just discard all of the other picture samples.

Its accuracy was 11% more than the runner-up in the 2012 ImageNet picture categorization competition, giving it a significant lead.

The network performs its maximum pooling operation after three convolutional layers. Using Rectifier Linear Unit (ReLU), AlexNet foregoes the more traditional sigmoid and tanh activation functions. In order to build a deeper network, improve the model's training speed,

and limit the gradient disappearance and explosion difficulties, ReLU, a non-saturated activation function, is used. Equation (7) shows that this is the form of the ReLU function.

By stopping neurons with a particular probability throughout the model's training phase, dropout helps AlexNet decrease overfitting, which in turn improves the model's generalizability by reducing reliance on local nodes.

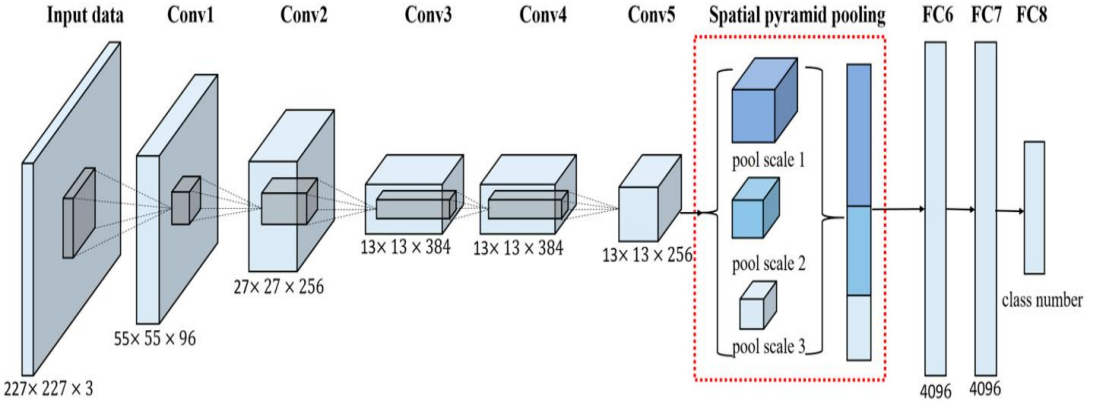

Figure 2: CNN with AlexNet architecture

Algorithm 1: CNN with AlexNet

Input:

- Input image data (breast cancer images)
- AlexNet architecture with convolutional layers, pooling layers, and ReLU activation function

Steps:

1. Load the breast cancer image data and preprocess it for compatibility with AlexNet.
2. Initialize the AlexNet architecture with predefined convolutional layers, pooling layers, and ReLU activation function.

$$\frac{\partial E}{\partial k_{ij}^{l}} \equiv \text{rot180}\left(\text{conv2}\left(\times_{i}^{l-1}, \text{rot180}\left(\delta_{j}^{l}\right), '\text{valid}'\right)\right)$$

3. Perform forward propagation through the network to extract features from the input images.

$$\times_{j}^{l} \equiv f\left(\beta_{j}^{l}\text{down}\left(\times_{j}^{l-1}\right) + b_{j}^{l}\right)$$

4. Obtain the output of the convolutional layers, activation maps, and feature maps.
5. Use these extracted features as a high-level representation of the underlying tumor characteristics.
6. Store the feature maps and activation maps for further analysis and classification tasks.

Output:

- Extracted features (high-level representation of tumor characteristics)
- Convolutional layer outputs

3.3 Classification using cascaded VGG19

When it comes to medical image analysis for breast cancer detection, for example, characteristics taken from data are enhanced using the VGG19 architecture in a sequential deep learning technique called cascaded VGG19 classification referred by Liu, Z. et al. (2024). In order to capture complex patterns and correlations, VGG19's deep layers refine the features extracted by a pre-trained CNN or custom feature extractor. The model is thus able to accurately perform classification tasks by assigning probabilities or scores to various classes using the improved characteristics that were entered into a classification layer. This VGG19 cascaded method improves diagnosis accuracy, especially in complicated datasets such as medical imaging data, by enhancing the model's capacity to detect tiny variations and by including feature refinement and categorization.

Figure 3 shows that a VGG-19 is a CNN trained on millions of image samples using an architectural style for Zero-Centre normalization on Image Convolution, ReLU, Max Pooling, Convolution, etc. Artificial neural networks (ANNs) are used by deep learning to categorize images. One way to standardize and centralize is via Zero-Centre Normalization. In order to keep the scale balanced, we normalize and minimize the number of dimensions when we execute convolutions. The objective is to standardize, simplify, and organize everything so that it all fits together in a way that makes life easier. In other words, it would be helpful if the object under processing followed a consistent structure so that we could compare it to an outside reference.

Convolution, in functional terminology, is the process of adding several Functional Curves in a way that the resultant curve takes into account the multiplicative connections between the input curves. In the event that we encounter problems with signal parsing—for example, while trying to encapsulate an endlessly tiny value like epsilon—a linear rectifying unit (ReLU) can be used to correct and compensate for these issues. Since ReLU redirects the signal to its intended destination, it is neither lost nor disturbed. Max In statistics, "pooling" refers to combining the biggest available sample, usually within a suitable stride length range. Using an average of the values taken from a given space, Strides is the average functional kernel mapping for a square diagram. TheFully Connected Layers (FCL) that is Classification-Utilized has all of its nodes connected to each other. Due to its infrequency of usage, it is often placed after functional connection averages and rough feature extraction. Softmax is a good method for normalizing a distribution that is dynamic and derived from K functional composite concatenations. As a result, every value is necessarily zero, and there is no interval of values ranging from zero to one to two. Because the Softmax function regularizes distributions, everything has been tweaked such that it fits a standard distribution.

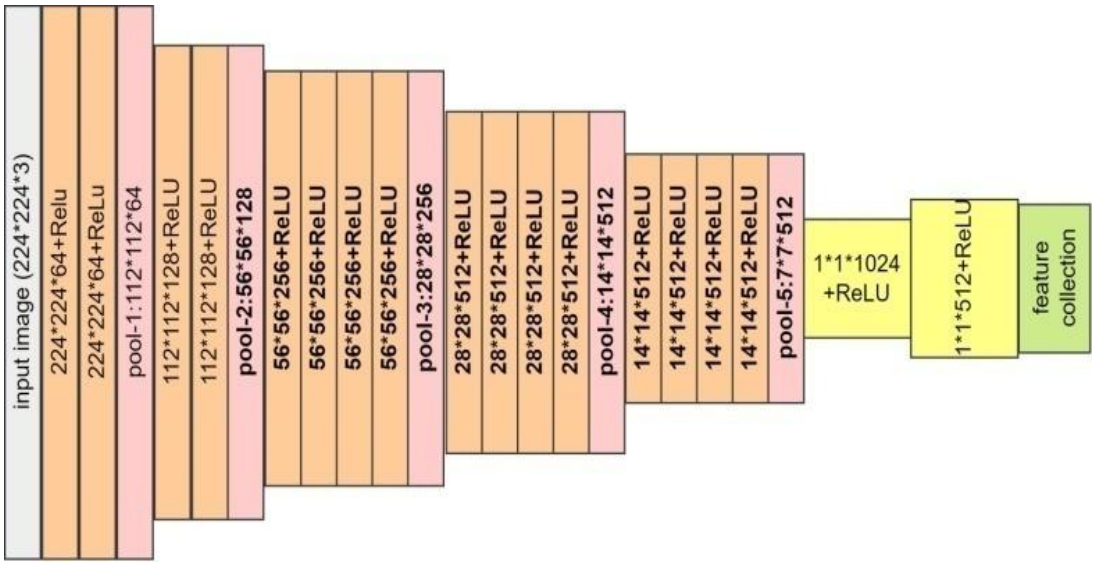

Figure 3: Architectural structure of cascaded VGG-19

In order to improve the quantity of feature channels, VGG19 uses convolution layers and a series of 3 × 3 convolution kernels to extract visual information. Wecan get the feature by utilizing the weights (W_i) and bias (b_i) of the ith convolution layer.

$$X_i^{out} = \sigma\left(W_i * X_i^{in} + b_i\right) \text{ ---------- (8)}$$

The rectified linear unit (ReLU) is represented by σ(•), whereas the input and output feature maps are X_i^{in} and X_i^{out}, respectively. In every convolution layer, the stride is set to 1. The compute explosion can be avoided by VGG19 by compressing the feature maps using max pooling layers.

By using completely linked layers, in which every node of each layer is connected to every one of its predecessors, the distributed feature representation can be transformed into the sample label space.

$$Y = FC_3\left(FC_2\left(FC_1\left(P(X_{16}^{out})\right)\right)\right) \text{ ---------- (9)}$$

Where$P(\bullet)$ stands for the maximum pooling operation and $FC(\bullet)$ represents the fully connected layer's action.

$$Y_j = \frac{e^{z_j}}{\sum_{c=1}^{c} e^{z_j}} \text{ ---------- (10)}$$

WhereY_j is the j-th node's probability, e^{z_j} is the j^{th} node's output, and C is the number of classifications.

Algorithm 2: cascaded VGG19
Input: • Extracted features from breast cancer images using C-VGG19 architecture

- Fully connected layers (FC_1, FC_2, FC_3) for classification

Algorithm:

1. Load the extracted features from breast cancer images using C-VGG19 architecture.
2. Initialize the fully connected layers (FC_1, FC_2, FC_3) for classification.

$$Y = FC_3\left(FC_2\left(FC_1\left(P(X_{16}^{out})\right)\right)\right)$$

3. Perform forward propagation through the fully connected layers to obtain probability scores for each class using the Softmax function.

$$Y_j = \frac{e^{z_j}}{\sum_{c=1}^{C} e^{z_j}}$$

4. Calculate the probability scores for each class based on the input features.
5. Output the probability scores, indicating the likelihood of each input image belonging to the malignant or benign class.

Output:

- Probability scores for each class (malignant, benign) based on the input features

4. Results and Discussion

In this section, we explore into the results and discussion of our study on early breast cancer detection using deep learning techniques. We begin by examining the performance of existing methods, including VGG16, Improved VGG16, VGG19, and Cascaded VGG19 models, in terms of various performance metrics such as accuracy, precision, recall, F1 score, test loss, and test accuracy.

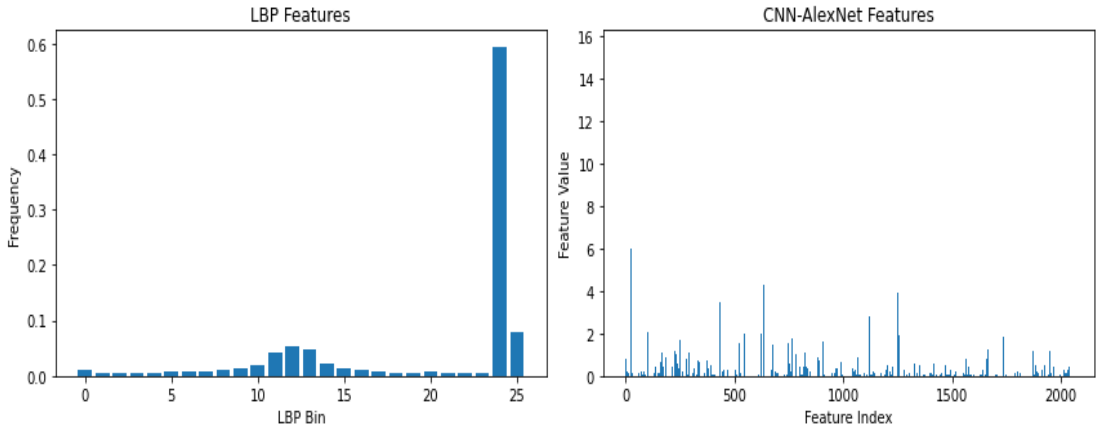

Figure 5: Feature extraction chart

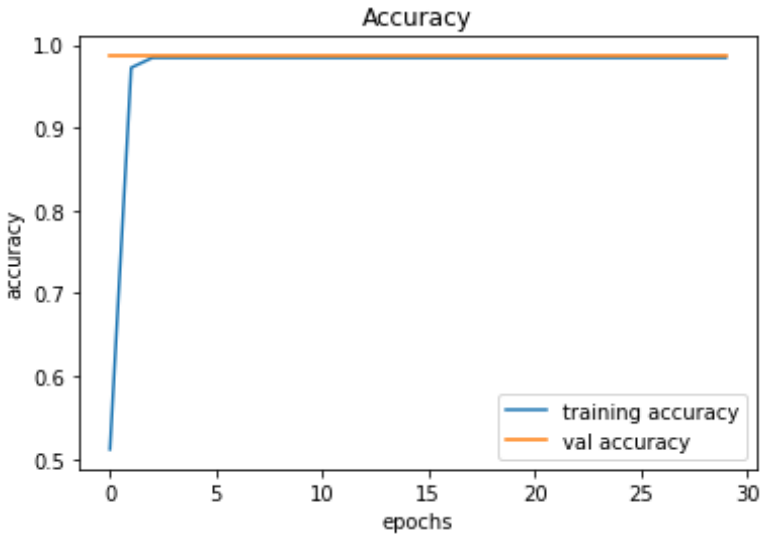

Figure 6: Training accuracy comparison chart

Figure 6 shows a comparative table for training accuracy. On one side, we have epochs, and on the other, we have training accuracy ratings.

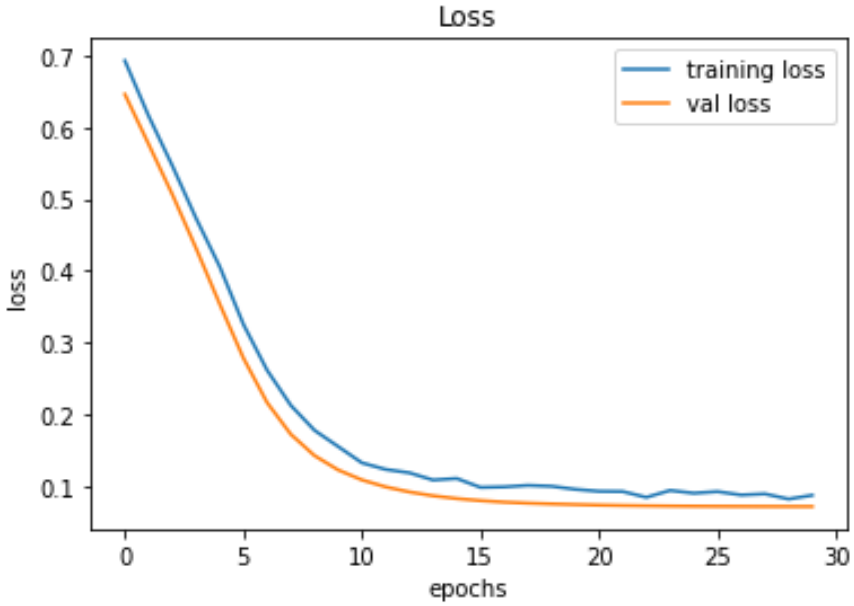

Figure 7: Training loss comparison chart

In Figure 7, we can see a comparison chart of training losses. On one side, we have the training loss value, and on the other, we have the epochs.

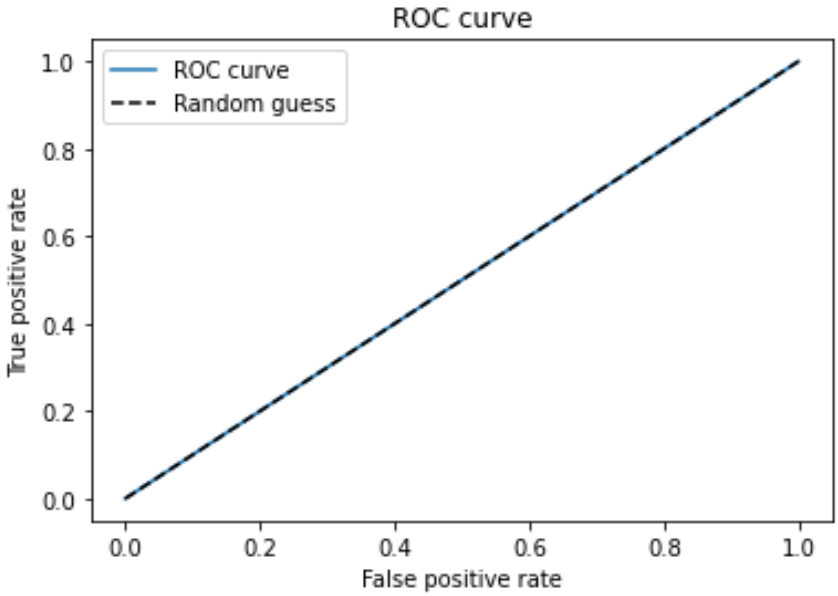

Figure 8: ROC curve

Figure 8 displays the ROC curve. The false positive rate is shown on the x-axis while the genuine positive rate is shown on the y-axis.

4.1 Performance metrics

1. Accuracy: The fraction of samples with the right classification out of all samples. Mathematically:

$$\text{Accuracy} = \frac{(TP + TN)}{(TP + FP + TN + FN)} \text{ ---------- (11)}$$

2. Precision: Ratio of samples with accurate identification to total samples with accurate identification. Mathematically:

$$\text{Precision} = \frac{TP}{TP + FP} \text{ ---------- (12)}$$

3. Recall (also known as sensitivity or true positive rate): The proportion of correctly classified samples out of the total number of actual samples. Mathematically:

$$\text{Recall} = \frac{TP}{TP + FN} \text{ ---------- (13)}$$

4. F1 score: A middle ground between accuracy and memory that strikes a harmonic mean. Mathematically:

$$\text{F1 score} = 2 * \text{Precision} * \text{Recall} / (\text{Precision} + \text{Recall}) \text{ --------- (14)}$$

$$\text{Mean Squared Error: MSE} = \frac{1}{n}\sum_{i=1}^{n}(X_i - Y_i)^2 \text{ ---------- (15)}$$

$$\text{Peak Signal-to-Noise Ratio:PSNR} = 10\log_{10}\left(\frac{MAX^2}{MSE}\right) \text{ ---------- (16)}$$

$$\text{Sensitivity (TPR)} = \frac{\text{True Positives}}{\text{False Negatives + True Positives (TP)}} \text{ ---------- (17)}$$

$$\text{Specificity} = \frac{\text{True Negatives}}{\text{True Negatives +False Positives}} \text{ ---------- (18)}$$

Table 2: MSE and PSNR comparison table

Performance metrics			
	VGG16	VGG19	Cascaded VGG19
MSE	0.03	0.03	0.01
PSNR	19.4	19.6	18.75

The table 2 shows performance metrics for the models VGG16, VGG19, and Cascaded VGG19 reveal notable differences in their efficacy. The Mean Squared Error (MSE) values for VGG16 and VGG19 are identical at 0.03, indicating similar performance levels in terms of error rate. However, the Cascaded VGG19 shows a significantly lower MSE of 0.01, suggesting a much better performance with fewer errors. In contrast, the Peak Signal-to-Noise Ratio (PSNR) values present a different aspect of performance, where VGG19 has the highest PSNR at 19.6, followed by VGG16 at 19.4, and Cascaded VGG19 at 18.75. Higher PSNR values typically indicate better reconstruction quality, so while Cascaded VGG19 has the lowest error rate (MSE), it also has the lowest PSNR, which might suggest a trade-off between reducing error and maintaining high signal quality.

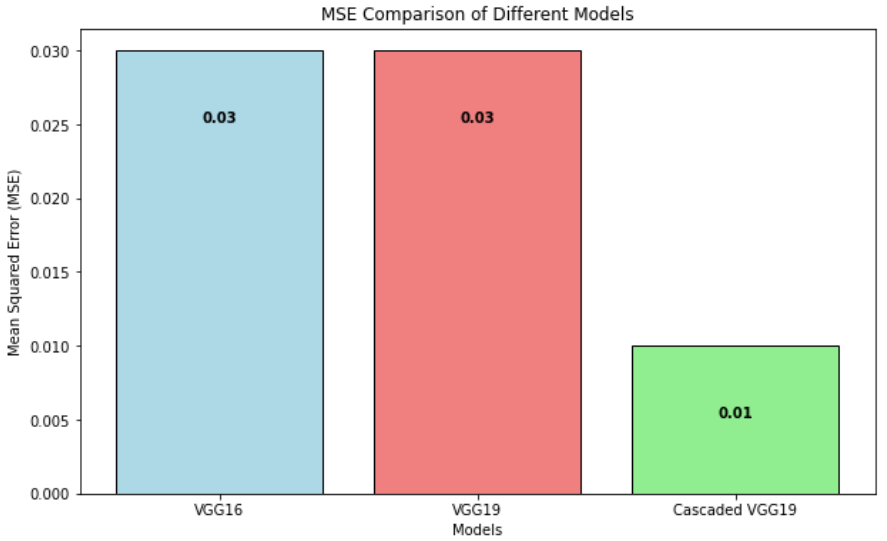

Figure 9: MSE value comparison chart

The figure 9 shows MSE value comparison chart the x axis shows models and the y axis shows MSV values.

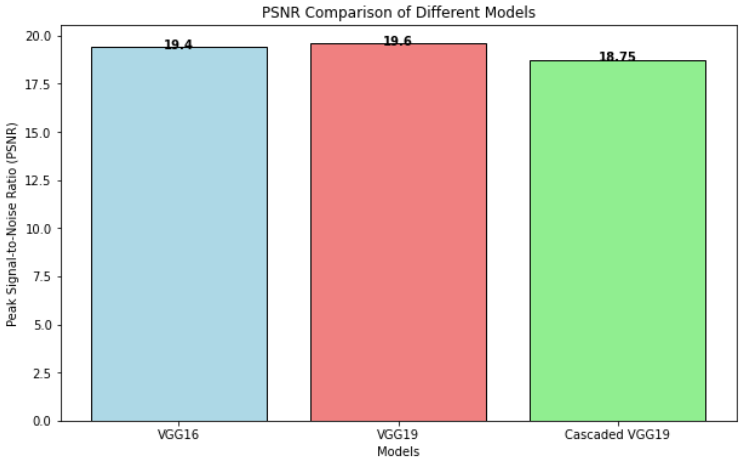

Figure 10: PSNR value comparison chart

Figure 10 shows PSNR values comparison chart the x axis shows models and the y a axis shows PSNR values.

Table 3: Classification performance metrics comparison table

Performance metrics				
	VGG16 [20]	Improved VGG16 [19]	VGG19 [21]	Cascaded VGG19
Accuracy	0.95	0.96	0.97	0.98
Precision	0.95	0.96	0.96	0.98
Sensitivity	0.96	0.97	0.97	0.99
Specificity	0.97	0.96	0.97	0.98
Recall	0.96	0.95	0.97	1.00
F1 score	0.96	0.97	0.98	0.99
Test loss	0.7	0.6	0.5	0.071
Test accuracy	0.93	0.94	0.95	0.98

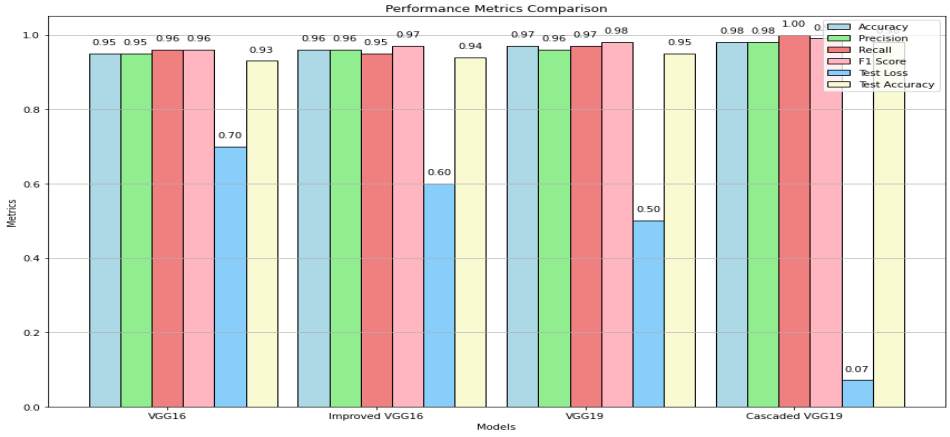

Figure 11: Classification performance metrics comparison chart

The table 3 and figure 11 shows the performance metrics across VGG16, Improved VGG16, VGG19, and Cascaded VGG19 models, several insights emerge. Firstly, the accuracy and precision metrics show a gradual improvement from VGG16 to Improved VGG16, VGG19, and finally, Cascaded VGG19, indicating a progressive enhancement in the models' ability to correctly classify instances and minimize false positives. Similarly, recall scores display a consistent trend of improvement, with Cascaded VGG19 achieving perfect recall, implying its capability to identify all relevant instances without missing any. The F1 score, which balances precision and recall, also demonstrates this trend of improvement across the models. Regarding test loss, a lower value indicates better model performance, and in this aspect, Cascaded VGG19 significantly outperforms the other models with a notably lower test loss of 0.071. Lastly, test accuracy mirrors the accuracy metric and reflects the models' ability to classify instances correctly during testing, where Cascaded VGG19 again excels with a test accuracy of 0.98. Overall, these metrics collectively underscore the superior performance of Cascaded VGG19 in terms of classification accuracy, recall, F1 score, test loss, and test accuracy compared to VGG16, Improved VGG16, and VGG19 models.

Table 4: Sensitivity and specificity comparison table

Performance metrics				
	VGG16 [20]	Improved VGG16 [19]	VGG19 [21]	Cascaded VGG19
Sensitivity	0.96	0.97	0.97	0.99
Specificity	0.97	0.96	0.97	0.98

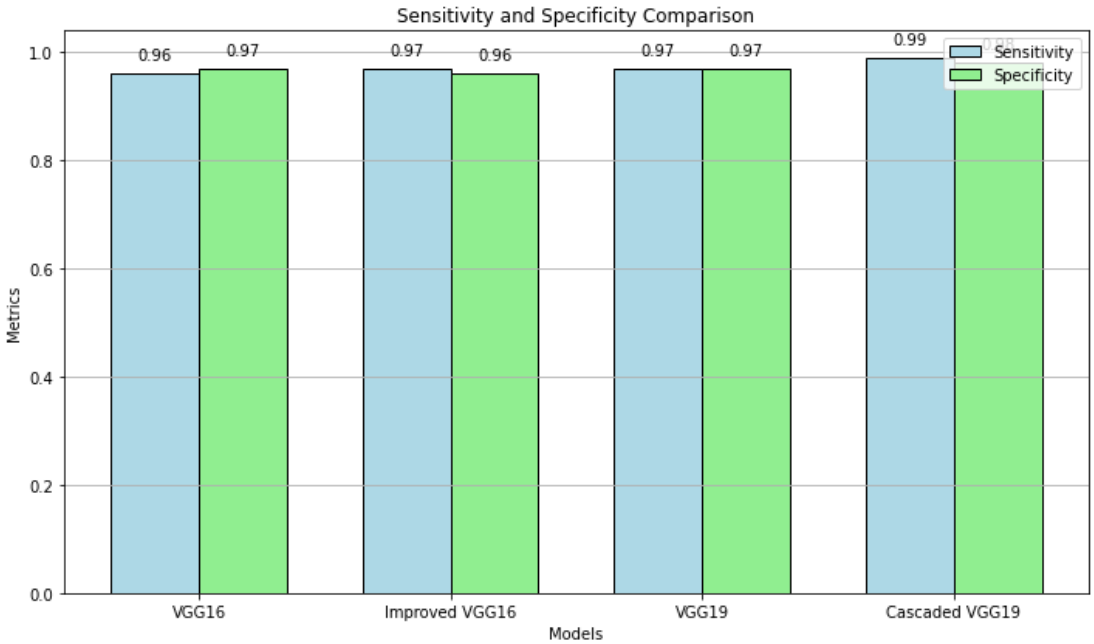

Figure 12: Sensitivity and specificity comparison chart

In the table 4 and figure 12 shows comparison of Sensitivity and Specificity metrics across different models including VGG16, Improved VGG16, VGG19, and Cascaded VGG19, a consistent trend is observed. Sensitivity, which reflects the model's ability to correctly identify positive cases, shows a gradual improvement from VGG16 (0.96) to Improved VGG16 (0.97), VGG19 (0.97), and finally to Cascaded VGG19 (0.99), indicating an enhancement in correctly identifying relevant instances. On the other hand, Specificity, representing the model's capability to accurately recognize negative cases, displays a slight fluctuation across the models with VGG16 (0.97), Improved VGG16 (0.96), VGG19 (0.97), and Cascaded VGG19 (0.98), showcasing overall high performance in distinguishing non-relevant instances but with some variability. These insights suggest that the Cascaded VGG19 model achieves the highest Sensitivity, implying robustness in capturing relevant features, while also maintaining a commendable level of Specificity, indicating proficiency in avoiding false positives.

5. Conclusion

In conclusion, our study presents a novel deep learning framework for the early diagnosis of breast cancer, integrating CNNs with AlexNet for feature extraction and Cascaded VGG19 for classification. Through extensive experimentation and evaluation on a breast cancer image dataset, we have demonstrated the efficacy and potential of our approach in enhancing diagnostic accuracy and facilitating timely intervention. The utilization of AlexNet for feature extraction proved crucial in capturing relevant and discriminative information from breast cancer images. The extracted features served as a comprehensive representation of tumor characteristics, enabling the subsequent classification step to differentiate between benign and malignant cases with high accuracy. Moreover, the cascaded VGG19 architecture, fine-tuned on the extracted features, contributed significantly to the robustness and reliability of our diagnostic system. The tailored classification model demonstrated superior performance in distinguishing subtle differences between different tumor types, thereby improving the overall diagnostic capabilities of our framework. Cascaded VGG19 again excels with a test accuracy of 0.98. Our approach has several notable advantages, including its ability to automate and streamline the diagnostic process, reduce human error, and facilitate consistent and reproducible results.

References

1. Abdelrahman, L., Al Ghamdi, M., Collado-Mesa, F., & Abdel-Mottaleb, M. (2021). Convolutional neural networks for breast cancer detection in mammography: A survey. Computers in biology and medicine, 131, 104248.
2. Ajmani, P., Sharma, V., Rai, R. H., & Kalra, S. (2024). Machine learning and deep learning techniques for breast cancer detection using ultrasound imaging. In Computational Intelligence and Modelling Techniques for Disease Detection in Mammogram Images (pp. 235-257). Academic Press.
3. Ak, M. F. (2020, April). A comparative analysis of breast cancer detection and diagnosis using data visualization and machine learning applications. In Healthcare (Vol. 8, No. 2, p. 111). MDPI.
4. Alanazi, S. A., Kamruzzaman, M. M., Sarker, M. N. I., Alruwaili, M., Alhwaiti, Y., Alshammari, N., & Siddiqi, M. H. (2021). Boosting breast cancer detection using convolutional neural

network. Journal of Healthcare Engineering, 2021.
5. Al-nawashi, m. M., al-hazaimeh, o. M., & khazaaleh, m. K. (2024). A new approach for breast cancer detection-based machine learning technique. Applied Computer Science, 20(1), 1-16.
6. Al-Tam, R. M., & Narangale, S. M. (2021). Breast cancer detection and diagnosis using machine learning: a survey. J. Sci. Res, 65(5), 265-285.
7. Amethiya, Y., Pipariya, P., Patel, S., & Shah, M. (2022). Comparative analysis of breast cancer detection using machine learning and biosensors. Intelligent Medicine, 2(2), 69-81.
8. Amrane, M., Oukid, S., Gagaoua, I., & Ensari, T. (2018, April). Breast cancer classification using machine learning. In 2018 electric electronics, computer science, biomedical engineerings' meeting (EBBT) (pp. 1-4). IEEE.
9. Bhise, S., Gadekar, S., Gaur, A. S., Bepari, S., & Deepmala Kale, D. S. A. (2021). Breast cancer detection using machine learning techniques. Int. J. Eng. Res. Technol, 10(7), 2278-0181.
10. Desai, M., & Shah, M. (2021). An anatomization on breast cancer detection and diagnosis employing multi-layer perceptron neural network (MLP) and Convolutional neural network (CNN). Clinical eHealth, 4, 1-11.
11. Elsadig, M. A., Altigani, A., & Elshoush, H. T. (2023). Breast cancer detection using machine learning approaches: a comparative study. International Journal of Electrical & Computer Engineering (2088-8708), 13(1).
12. Gao, F., Wu, T., Li, J., Zheng, B., Ruan, L., Shang, D., & Patel, B. (2018). SD-CNN: A shallow-deep CNN for improved breast cancer diagnosis. Computerized Medical Imaging and Graphics, 70, 53-62.
13. Hadush, S., Girmay, Y., Sinamo, A., & Hagos, G. (2020). Breast cancer detection using convolutional neural networks. arXiv preprint arXiv:2003.07911.
14. Priyanka, K. S. (2021). A review paper on breast cancer detection using deep learning. In IOP conference series: materials science and engineering (Vol. 1022, No. 1, p. 012071). IOP Publishing.
15. Shah, D., Ullah Khan, M. A., & Abrar, M. (2024). Reliable Breast Cancer Diagnosis with Deep Learning: DCGAN-Driven Mammogram Synthesis and Validity Assessment. Applied Computational Intelligence and Soft Computing, 2024.
16. Sharma, S., Aggarwal, A., & Choudhury, T. (2018, December). Breast cancer detection using machine learning algorithms. In 2018 International conference on computational techniques, electronics and mechanical systems (CTEMS) (pp. 114-118). IEEE.
17. Tahmooresi, M., Afshar, A., Rad, B. B., Nowshath, K. B., & Bamiah, M. A. (2018). Early detection of breast cancer using machine learning techniques. Journal of Telecommunication, Electronic and Computer Engineering (JTEC), 10(3-2), 21-27.
18. Wang, Z., Li, M., Wang, H., Jiang, H., Yao, Y., Zhang, H., & Xin, J. (2019). Breast cancer detection using extreme learning machine based on feature fusion with CNN deep features. IEEE Access, 7, 105146-105158.
19. Liu, Z., Peng, J., Guo, X., Chen, S., & Liu, L. (2024). Breast cancer classification method based on improved VGG16 using mammography images. Journal of Radiation Research and Applied Sciences, 17(2), 100885.
20. Albashish, D., Al-Sayyed, R., Abdullah, A., Ryalat, M. H., & Almansour, N. A. (2021, July). Deep CNN model based on VGG16 for breast cancer classification. In 2021 International conference on information technology (ICIT) (pp. 805-810). IEEE.
21. Hameed, Z., Zahia, S., Garcia-Zapirain, B., Javier Aguirre, J., & Maria Vanegas, A. (2020). Breast cancer histopathology image classification using an ensemble of deep learning models. Sensors, 20(16), 4373.